

ON ENCAPSULATING AND DELIVERY OF POLYPHENOLS IN SUPERPARAMAGNETIC POLYMER NANOSPHERES♦

Vasile Bădescu^{1*}, Laura E. Udrea¹, Ovidiu Rotariu¹,
Rodica Bădescu², Gabriela Apreotesei²

¹ *National Institute of Research and Development for Technical Physics,
47 Mangeron Blvd., Iași, 700050, Romania*

² *Technical University “Gh. Asachi”, Department of Physics,
67 Mangeron Blvd., Iași, 700050, Romania*

*Corresponding author: bav08@phys-iasi.ro

Received: 18/04/2008

Accepted after revision: 11/06/2008

Abstract: In this work we report on an encapsulating and delivery study of a red grape skins antioxidant extract (polyphenols) in a superparamagnetic composite matrix. The encapsulating matrixes used were sodium alginate base aqueous ferrofluid, obtained by an *in situ* precipitation of magnetite, and chitosan in acetic acid.

Red grape skins lyophilized extracts were encapsulated with two different systems: calcium alginate and calcium alginate–chitosan. FT-IR spectra were useful to confirm the interaction of the two polysaccharides. DLS measurements allowed determining the average size and size distribution of the polymeric nanoparticles encapsulating polyphenols. Transmission electron microscopy (TEM) of nanoparticles allowed studying their

♦ Paper presented at the fifth edition of: “Colloque Franco-Roumain de Chimie Appliquée – COFrRoCA 2008”, 25 – 29 June 2008, Bacău, Romania.

morphology and polydispersity.

Release of the antioxidants in water was measured to analyze the diffusion and kinetic behavior of the system. Different matrix destabilizing agents (HCl 0.1 N, NaOH 0.1 N and sodium citrate 1 and 10% w/v as a calcium chelator at ambient temperature, and distilled water at 50 and 100 °C) were tested. Sodium citrate was found to be the most effective agent to disintegrate the beads.

Superparamagnetic polymer nanoparticles encapsulating polyphenols opens up avenues for targeted therapy of some human diseases that are in part a result of free radical damage.

Keywords: *encapsulating, polyphenols, superparamagnetic nanocomposite, release kinetics.*

INTRODUCTION

Encapsulation is a process in which thin films, generally of polymeric materials, are applied to little solid particles, liquid or gases droplets. This method is used to trap active components and release them under controlled conditions. Several materials have been encapsulated in the food and pharmaceuticals industry, among others, aminoacids, vitamins, minerals, antioxidants, colorants, enzymes and sweeteners.

Polyphenols are antioxidants that have become increasingly recognized as possible combatants of the dangerous free radicals that threaten the well being of the human organism. There are promise that polyphenols are efficacious and safe compounds for cancer therapy and chemoprevention. The development of a delivery system that can enable parenteral or intravenous administration of polyphenols in an aqueous phase medium will significantly harness the potential of this promising anti-cancer agent in the clinical arena. Also, the targeting of therapeutic compounds in the tumor zone, for the locally and programmed delivery of drug is at this time a challenge. Superparamagnetic carrier nanoparticles represent an increasingly important class of supports devices that provide enhanced control of biological entities. Comparatively with nonmagnetic polymer carriers, magnetic microbeads offer still an additional advantage: having embedded magnetic entities, they can be magnetically controlled in time and space, using permanent magnets or electromagnets. Magnetic carriers realized from natural polymers have advantages of being used in very interesting areas such as biomedicine and biotechnology, because of their properties like very good biocompatibility, biodegradability and the feasibility to incorporate drugs/enzymes into their matrices.

In this work, lyophilized extracts of red grape skins were encapsulated in a superparamagnetic composite matrix. The encapsulating agents used in this study were sodium alginate base aqueous ferrofluid, obtained by an *in situ* precipitation of magnetite, and chitosan in acetic acid. Chitosan and alginate can react together by coacervation due to their opposite charges, alginate - chitosan complexes solve some limitations of individual polyelectrolytes [1, 2]. The easy solubility of chitosan at low *pH* is prevented by the alginate network since alginate is insoluble at low *pH* conditions. The possible dissolution of alginate at higher *pH* is prevented by the chitosan, which is stable at higher *pH* ranges.

We report on the synthesis, physico-chemical characterization and release of active factor from superparamagnetic carriers consistently in size less than 100 nm.

MATERIALS AND METHODS

For obtaining superparamagnetic nanocapsules, we have gelatinised nanodrops of an alginate ferrofluid, prepared by a known synthetic scheme [3]. Briefly, alginate polymer (Merck, Germany) was cross-linked by ferrous ions in a water/methanol 0.1 M solution of FeCl_2 (Merck, Germany), followed by precipitation of iron hydroxide with sodium hydroxide and finally oxidation to iron oxide. Magnetic alginate flakes of 2-3 μm size were formed. The exposure of the flakes to the cycle $\text{Fe}^{2+}/\text{NaOH}/\text{oxidation}$ was repeated up to six times, leading to a high level of iron incorporation within the alginate flakes (up to 25% Fe w/w). At the end of the cycles, the magnetic gel alginate flakes were removed from the methanol/water suspending medium by decantation. They were dispersed in water and subjected to sonication at 25 °C for 1 h. The resulting suspension was treated with aqueous sodium phosphate and sonicated for 30 min to complete the disintegration of the flakes. The mixture was purified by centrifugation to remove insoluble residues and excess alginate. The supernatant was concentrated by ultra-centrifugation and filtered through a 0.25 μm membrane, obtaining the final aqueous ferrofluid, a superparamagnetic alginate solution. The size distribution of magnetite nanoparticles in aqueous ferrofluid was obtained by dynamic light scattering (DLS). The analysis shows a log-normal distribution, with particles having an average diameter of 15.6 nm. The magnetization curve of ferrofluid is presented in Figure 1. The ferrofluid behaves as a superparamagnetic material, this character being important for biotechnological and biomedical applications were a remanent magnetization is undesirable. For such applications, the particles must rapidly relax their magnetic moment vectors to random directions when the applied magnetic field is removed.

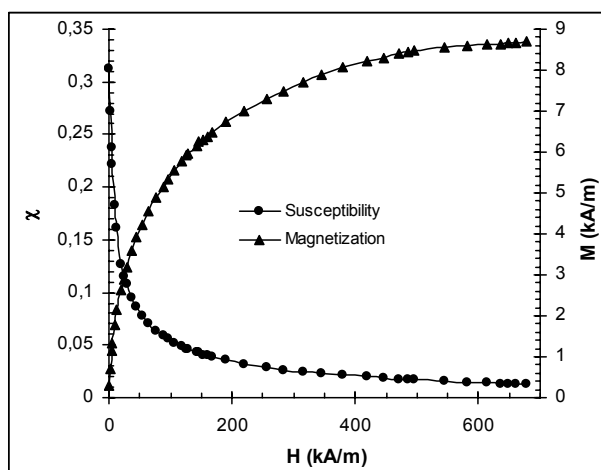


Figure 1. The magnetic properties of the aqueous ferrofluid

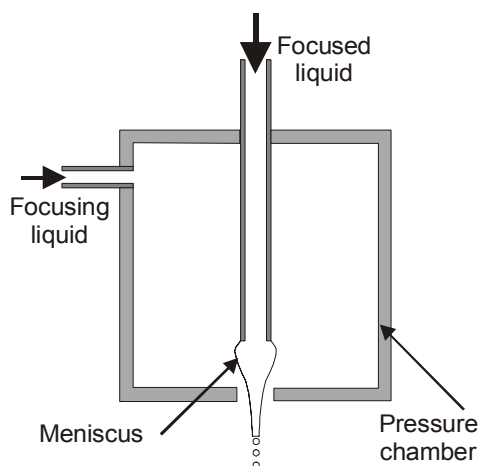


Figure 2. Flow-focusing apparatus.

The superparamagnetic alginate-polyphenols nanocapsules were produced as follows:

various percentages of ferrofluid were mixed with a 1.5% (w/v) alginate solution and a solution of active component (1% w/v). The mixtures were used as disperse phase for atomization in a flow-focusing system, the continuous phase being a solution of 5% sorbitan monooleate in isooctane (Aldrich, Germany). The resulting alginate ferrofluid micro-jet break-up into nanodroplets dispersed in isooctane.

Flow-focusing consist on an atomization technique, which relies on hydrodynamic forces to produce microjets [4]. In this method, a flow rate Q is injected through a capillary needle. This needle is placed inside a pressure chamber as sketched in Figure 2. The liquid disperse phase is injected through the needle, giving rise to a meniscus at the extremity of the needle. An orifice in the chamber wall facing the tip of the needle opens the camber to the outer ambient. The continuous phase is forced to escape the camber through the orifice by means of an extra pressure in the camber. When this reaches a certain value, the surface tension stress at the meniscus are overcome, so that it is pulled into a cusp-like shape from whose vertex a very slender micro-jet issues with diameter smaller than inner diameter of the needle.

Once the micro-jet exits the orifice, the pressure gradient (the main axially accelerating force) vanishes and the jet evolves under the influence of the viscous shear stress produced by the continuous phase stream and the capillary stresses. Perturbations of the capillary jet grow downstream until the jet breaks up.

Our experimental data were obtained with an atomizer for which the inner diameter of the needle was 19 μm , the diameter of the orifice in the wall chamber was 150 μm and the thickness of the wall chamber was 50 μm . Most experimental data were obtained varying the continuous phase flow rate between 0.07 and 0.17 mL/min while maintaining the disperse phase flow rate of 0.004 mL/min.

The w/o superparamagnetic emulsion was stirred gently for 30 min to develop a stable emulsion. Then a calcium chloride solution was added for cross-linking the alginate magnetic nanospheres. The nanospheres were filtered, washed and allowed to stabilize in air for different times (0 – 40 min), forming control samples. To analyze the effect of an additional layer, nanospheres were immersed in the chitosan solution for 0, 15, 30 or 60 min. The capsules were dried at ambient conditions, in an oven at 80 °C for 24 h and by freeze drying for 48 h, forming chitosan coated samples.

Analysis by Fourier transform infrared (FT-IR) spectroscopy was performed on the single components, sodium alginate and chitosan films, and on control and chitosan coated beads. A FT-IR spectrophotometer (Perkin Elmer) was used. Samples were scanned from 600 to 4000 cm^{-1} at a resolution of 4 cm^{-1} . DLS measurements for determining the average size and size distribution of the nanocapsules were performed using a Nanosizer 90 ZS, Malvern Instruments. SEM analysis was performed using a Jeol JSM-6360 microscope operating at magnification of 80 kV with 1 K \times 1 K digital images captured using an Sony CCD camera.

To test nanocapsules destabilization, known amounts (100 mg) of control and chitosan coated samples were dispersed in test tubes containing 10 mL of different destabilizing agents: HCl 0.1 N, NaOH 0.1 N and sodium citrate 1 and 10% w/v as a calcium chelator were assayed at ambient temperature, and distilled water was tested at 50 and 100 °C. Observations were performed for 24 h.

The amount of lyophilized extract loaded in nanocapsules was estimated by dissolving a known amount of samples in sodium citrate (10% w/v) during 20 min for control nanocapsules and 90 min for chitosan coated nanocapsules. A blank of sodium citrate

solution was also performed. The concentrations of lyophilized extract in solutions were measured spectrophotometrically at 450 nm. The percentage of loading efficiency was calculated with the following equation:

$$E(\%) = \frac{L}{L_0} \times 100 \quad (1)$$

where L is the amount of extract determined on the solution of sodium citrate and L_0 is the initial amount of extract dissolved in the alginate solution.

For testing the active agent release, known amounts (100 mg) of control and coated chitosan nanoparticles encapsulating polyphenols were dispersed in 10 mL distilled water and the solutions were divided each in 20 microfuge tubes (500 μ L). Free extract is completely insoluble in water; therefore, at predetermined intervals of time, the solutions were centrifuged at 3000 rpm for 10 minutes to separate the released (pelleted) extract from the loaded nanoparticles. The released extract was redissolved in 1 mL of ethanol and the absorbance was measured spectrophotometrically at 450 nm. The concentration of the released extract was then calculated using standard curve of extract in ethanol. The percentage of extract released was determined from the equation:

$$Release(\%) = \frac{C_{rel}}{C_{tot}} \times 100 \quad (2)$$

where, C_{rel} is the concentration of released extract collected at time t and C_{tot} is the total amount of extract entrapped in the nanoparticles.

RESULTS

In Figure 3a the typical size distribution of the nanoparticles is illustrated, and the average size corresponds to less than 100 nm diameter at 25 °C with a narrow size distribution. Transmission electron microscopy (TEM) of the nanospheres is illustrated in Figure 3b, and demonstrates that the particles have spherical morphology and low polydispersity with an approximate size of around 90 nm diameter, which is comparable to the size obtained from DLS measurements.

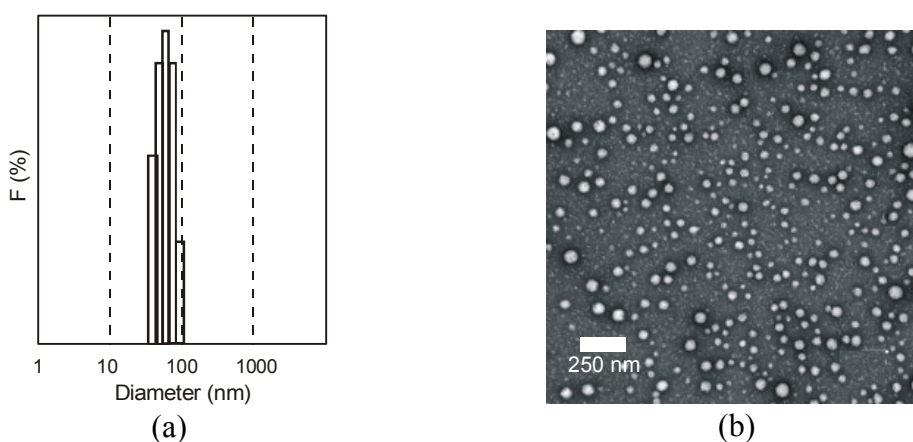


Figure 3. Size characterization of the superparamagnetic nanospheres: (a) using DLS; (b) using TEM

Hydrocolloids, sodium alginate and chitosan have similar structure so their FTIR spectra have characteristic bands attributed to their saccharide units (Fig. 4a and b). Between 3450 and 3490 cm^{-1} spectra show a band attributed to the $-\text{OH}$ groups; the glucose ring appears around 1060 and 1150 cm^{-1} . Chitosan has typical bands due to the amino and amide groups present in its structure. Control (c) and chitosan coated (d) beads, and alginate film showed similar spectra, this match was attributed to the high proportion of alginate in the capsules (Fig. 4). The band around 1050 cm^{-1} present in chitosan film arose in chitosan coated beads (d); this band is attributed to skeletal vibrations involving the CO stretching. Besides, new bands around 1117 and 1240 cm^{-1} were distinguished, indicating an electrostatic interaction between the protonated amino groups of chitosan and the dissociated carboxylate groups of sodium alginate, respectively. Wavenumber shifts of typical bands appearing in pure hydrocolloids (a and b) were also found in bead spectra: the band appearing at 1590 cm^{-1} in pure alginate was found at 1620 cm^{-1} in both type of beads.

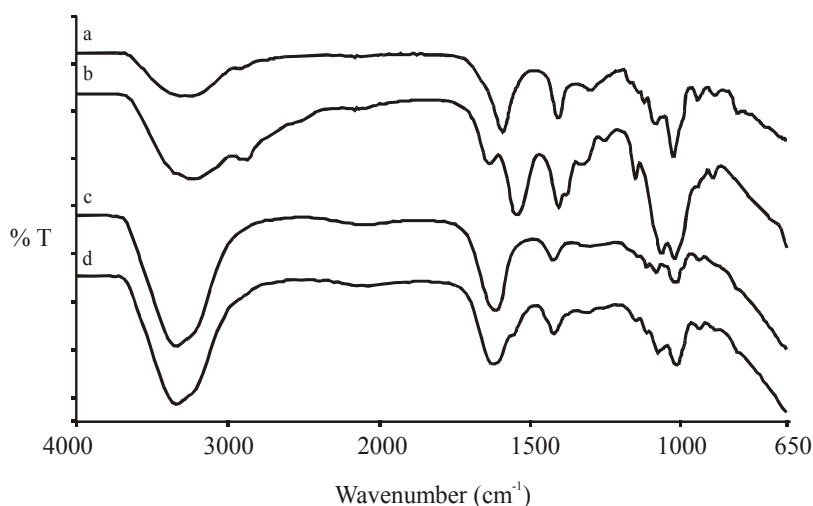


Figure 4. FT-IR spectra: (a) alginate film, (b) chitosan film, (c) control sample, (d) chitosan coated sample.

Destabilization of the encapsulation system is required for total release of the active compounds. Several conditions were analyzed: temperature, hydrochloric acid, sodium hydroxide and sodium citrate media. Sodium citrate destabilized the calcium alginate gel; Ca^{+2} ions of the network were exchanged by Na^{+} ions, weakening the gel structure. This destabilizing agent showed a lower effect on chitosan beads compared to control ones; after 20 min of immersion in the solution, control samples were dissolved and nanocapsules with chitosan remained intact. Ninety minutes were needed to disintegrate the chitosan coated nanocapsules.

Loading efficiencies of the two types of nanocapsules were significantly different (Table 1). Control samples showed a high load of active compound. In chitosan coated samples compound losses were produced during immersion in chitosan.

Percentage release was calculated based on the actual entrapped polyphenol extract (Table 1). The lower release of chitosan coated samples can be attributed to higher retention characteristics due to the alginate-chitosan membrane and the possible interaction between chitosan and polyphenols from extract.

Table 1. Efficiency of different encapsulation systems

Sample type	Parameters	
	Loading efficiency (%)	Release in water (%)
Control sample	87.4 ± 0.2	47.6 ± 0.3
Chitosan coated sample	48.5 ± 0.5	35.4 ± 0.2

Figure 5 shows *Release (%)* as a function of time. Two zones were distinguished, a first increasing zone and a last stage independent of time. The second zone characterized by a constant release rate was reached at 210 min for chitosan coated nanocapsules and at 300 min for control ones; this stage corresponded to a zero order mechanism.

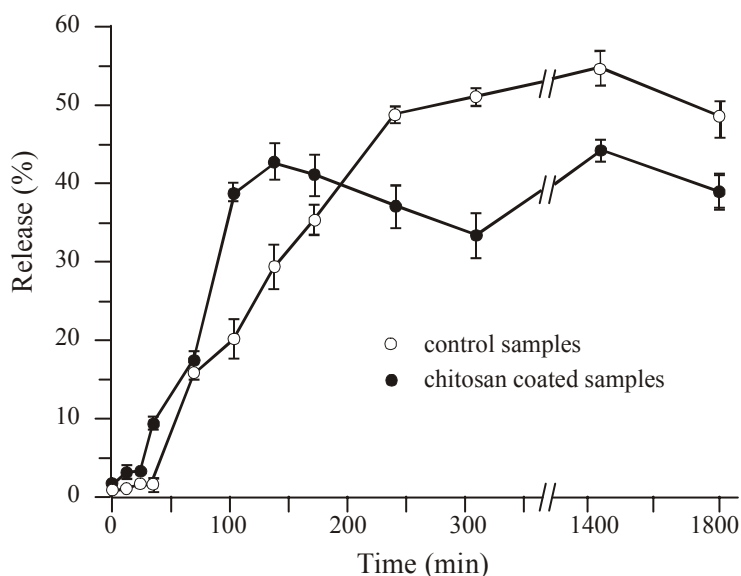


Figure 5. Release curve: C_{rel}/C_{tot} vs. time

To evaluate the release mechanism, a semi-empirical equation was applied to the first part of the kinetic curve:

$$\frac{C_{rel}}{C_{tot}} = kt^n \quad (3)$$

where k is a constant related to structural and geometric characteristics of the beads, and n is the exponent indicative of the release mechanism. These parameters were calculated using the relative release values corresponding to the time dependent part of the curve for each system. Both nanocapsule systems gave n values higher than 1, associated to different mechanisms acting together. As it is known, the parameter n can take a range of values indicating the type of transport of the active agent. When $n = 0.5$, the active agent is released by simple Fickian diffusion. When $n = 1.0$, diffusion is described as *case II* transport; in this case, the rate of solvent uptake by the polymer is largely determined by the rate of swelling and relaxation of the polymer chains. *Super case II* transport occurs when $n > 1.0$ and is related to the plasticization of the polymer system, a reduction of the attractive forces between chains that increases the mobility, thus the active compound release is facilitated. In our case, both systems behaved similarly, an initial chain plasticization that allowed diffusion and then a swelling and relaxation

mechanisms acting together. The fact that chitosan samples released a lower relative amount of antioxidant could be attributed to the interaction between polyphenols compounds and chitosan. Chitosan coated nanocapsules did not delay transport rate, as it was expected. Experimental observations showed that several chitosan coated nanocapsules, once dipped in water were disrupted. We attributed this behavior to the fracture of the external layer of chitosan owing to the higher relaxation and water uptake of the calcium alginate gel inside the chitosan - alginate layer of the nanocapsules.

CONCLUSIONS

High load of active compound (> 85%) was obtained in control samples. However, the entrapment in chitosan coated nanocapsules was lower (around 50%) since active compound was lost during immersion in chitosan. The percentage released was higher for control samples since polyphenols could be retained in chitosan–alginate membrane. However, maximum release in water was achieved at shorter times for chitosan coated samples compared with control ones. Diffusion behavior did not follow a Fickian model, a *Super case II* transport was observed in both encapsulating systems.

ACKNOWLEDGEMENTS

This study was supported by Grant 108/2006 of National Authority for Scientific Research, CEEEX – MATNANTECH Program, Romania.

REFERENCES

1. Gåserød, O., Sannes, A., Skjåk-Bræk, W.: Microcapsules of alginate–chitosan. II. A study of capsule stability and permeability, *Biomaterials*, **1999**, 20(8), 773-783;
2. George, M., Abraham, E.: Polyionic hydrocolloids for the intestinal delivery of protein drugs: Alginate and chitosan – a review, *Journal of Controlled Release*, **2006**, 114(1), 1-14;
3. Kroll, E., Winnik, F.M., Ziolo, R.F.: In Situ Preparation of Nanocrystalline γ -Fe₂O₃ in Iron(II) Cross-Linked Alginate Gels, *Chemistry of Materials*, **1996**, 8(8), 1594-1596;
4. Xu, S., Nie, Z., Seo, M., Lewis, P., Kumacheva, E., Stone, H., Garstecki, P., Weibel, D.B., Gitlin, I., Whitesides, G.M.: Generation of Monodisperse Particles by Using Microfluidics: Control over Size, Shape, and Composition, *Angewandte Chemie International Edition*, **2005**, 44(5), 724-728;
5. Pasparakis, G., Bouropoulos, N.: Swelling studies and in vitro release of verapamil from calcium alginate and calcium alginate–chitosan beads, *International Journal of Pharmaceutics*, **2006**, 323(1-2), 34-42.